

Application of Almost-everywhere Singular Distributions in Chemical Engineering

Massimiliano Giona and Oreste Patierno

Centro Interuniversitario sui Sistemi Disordinati e sui Frattali nell'Ingegneria Chimica, c/o Dip. Ingegneria Chimica, Università di Roma "La Sapienza," 00184 Rome, Italy

Almost-everywhere singular (AES) distributions, usually referred to as multifractal measures, provide an intermediate link between atomic distributions (distributions represented by a countable superposition of Dirac's delta terms) and smooth regular distributions. This article shows how AES distributions can be rigorously treated in connection with distributed-parameter models and presents closed-form expressions and/or recursive, uniformly converging approximation methods for integral transforms (Laplace and Stieltjes). In particular, exact results are obtained and discussed for linear and uniform nonlinear kinetics and for transport schemes in the presence of continuous mixtures. The physical origin of AES distributions in real systems is also detailed.

Introduction

In many different problems of chemical engineering, model formulation involves a continuous parametrization of the concentration of the reacting-diffusing species with respect to one or more parameters characterizing the mixture.

This is the case with all population-balance models (Himmelblau and Bishoff, 1968), cell population dynamics parametrized with respect to DNA or protein content (whose population distribution with respect to the parameter can be experimentally monitored with flow-cytometric methods), and in general with continuous kinetics and thermodynamics.

In particular, continuous kinetic modeling (see Astarita and Sandler (1991) for an overview), which has been extensively developed starting with the article by Aris and Gavalas (1966), provides a powerful alternative to discrete lumping in some cases.

No matter what particular application is involved, however, the mathematics of continuous distributions and the resulting chemical engineering applications have been developed in terms of the following main approaches:

- Either by considering atomic distributions, that is, distributions composed by at most a countable sequence of Dirac's delta terms

- Or by assuming smooth continuous distributions, such as the gamma distribution $\rho(x) = \lambda^{\beta+1} x^{\beta} \exp(-\lambda x) / \Gamma(\beta+1)$, $\beta > -1$, which is one of those most commonly used distributions in continuous kinetic literature.

The mathematical developments associated with the implications of fractal geometry (Mandelbrot, 1982) have opened up new perspectives in the treatment of distribution functions. Mandelbrot (1974, 1982, 1988) and Halsey et al. (1986) have highlighted the properties of almost-everywhere singular (AES) distributions, which are usually referred to as *multifractal* because they are characterized by a continuous spectrum of fractal dimensions related to their singularity structure (see Appendix 1). A more rigorous definition of AES distributions is presented in the next section.

Such distributions arise in connection with cascade or multiplicative processes, the simplest example being the binomial measure (Mandelbrot, 1982). Multifractal distributions appear in the study of the statistical properties of chaotic dynamical systems, and may explain the fine structure of turbulent eddies, as some writers suggest (e.g., Sreenivasan and Meneveau, 1986; see also Procaccia, 1984). They are also related to the distribution of stretching exponents in chaotic mixing (Muzzio et al., 1992a,b), and arise in many other natural processes (e.g., earthquakes) and manufacturing processes (e.g., fragmentation and traffic flow in computer networks), as extensively discussed by Mandelbrot (1982).

AES distributions are usually approached by means of scaling analysis, by introducing a spectrum of generalized dimen-

$$\rho(x) = \sum_{n=0}^{\infty} \rho_n \delta(x - x_n) \quad \sum_{n=0}^{\infty} \rho_n = 1, \quad (1)$$

Correspondence concerning this article should be addressed to M. Giona at: Dipartimento di Ingegneria Chimica, Università di Cagliari, piazza d'Armi, 09123 Cagliari, Italy.

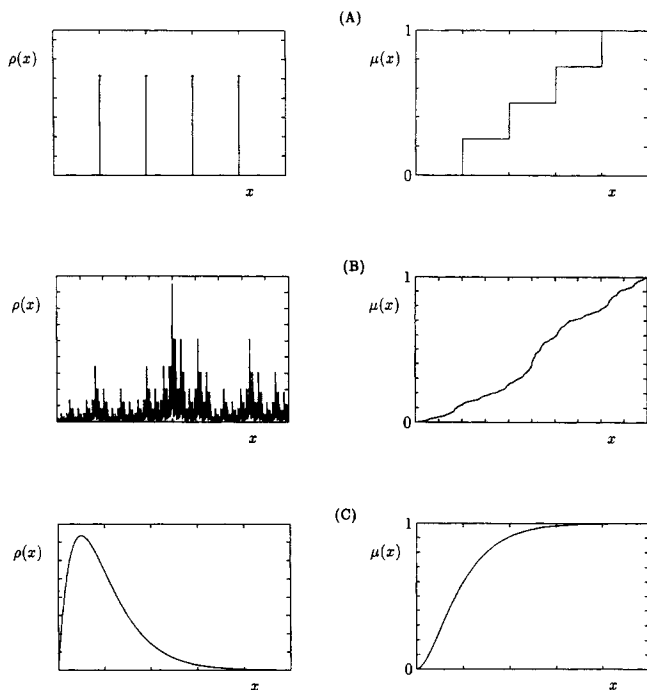


Figure 1. Difference between atomic (A), AES (B), and continuous (C) distributions in one dimension.

$\mu(x) = \mu([0, x])$ and $\rho(x)$ is the corresponding density function. The arrows in (A) indicate Dirac's delta contributions.

sions, or the so-called multifractal spectrum $f(\alpha)$. See the Appendix 1 for a very succinct overview of these concepts.

Figure 1 illustrates the distinction between atomic, AES, and continuous distributions.

In many situations, thermodynamic and kinetic properties depend on some smooth (or fictitiously continuous) parameter such as molecular weight, number of carbon atoms, or monomer number. In all these cases, the mixture can be described by means of a smooth distribution or by lumping the system with the introduction of a finite number of pseudo-components.

In other cases, however, there is no physical reason to assume regularity in the shape of distributions other than the mathematical solvability of model equations (since we are accustomed to handling smooth distributions by means of standard calculus, or discrete distributions within the theory of generalized functions). This is typically the case encountered in heterogeneous chemistry, where surface heterogeneity (e.g., dislocations and surface defects) and chemical heterogeneity may induce a very complex distribution of catalytic activities that can hardly be described by means of smooth functions. This problem is clearly highlighted by Gutfraind et al. (1990, 1991, and references therein) in connection with catalytic surfaces.

Moreover, in environmental processes involving fluid and solid wastes, treated either by adsorption or by incineration/gasification, the feed mixture composition may display a high level of heterogeneity, due, for example, to daily/seasonal fluctuations, which could be more satisfactorily described by means of distribution functions such as that shown in Figure 1b.

Another interesting example of highly singular mixtures is provided by Moore and Anthony (1989) in the case of diesel fuel (Figure 2 of Moore and Anthony), for which capillary-column gas-chromatograms of the mixture show such a high level of discontinuity that the application of continuous modeling is highly questionable. As noted by these authors, the highly singular structure of the diesel-fuel mixture is not suitable for the calculation techniques currently available. A way to overcome the mathematical problems posed by Moore and Anthony is developed in this article. The purpose of this work is not to discuss the scaling properties of AES distributions, but rather to show that AES distributions are well-defined mathematical objects (this point is, however, already established in the literature, e.g., by Falconer (1990)) that can be correctly and rigorously applied in a variety of chemical engineering and technological problems.

The article also presents new closed-form results for the corresponding Laplace and Fourier transforms of AES distributions as well as exact recursion schemes, making it possible to compute integral transforms accurately (as in the case of Stieltjes transforms).

As noted by Aris (1991), the theory of integral transforms is in fact the basic tool used in the mathematical development of the kinetics of continuous mixtures: Laplace transforms arise in batch processes, and Stieltjes transforms are connected with the analysis of continuous stirred-tank reactor (CSTR).

Attention is focused on reaction and transport processes involving continuous mixtures in which the distribution function of the species is described by AES distributions.

The article is organized as follows. The next section provides a brief review of the basic tools needed for rigorous and general treatment of AES distributions. We then show that integral transforms of AES distributions can be obtained in closed form. All these results are applied to a variety of problems: linear and nonlinear uniform kinetics for a continuous mixture and continuous lumping in a CSTR, as well as transport and adsorption schemes involving a continuous parametrization of the species. A detailed discussion on the physical origin of AES distributions in real systems is developed in the subsections titled "Reaction in Chaotic Mixing Systems" and "Nonstandard Transport Phenomena" in connection with reaction/diffusion in chaotic mixing systems. Some experimental evidence of real mixtures (pollutant distributions) showing a highly singular structure qualitatively similar to that of AES distributions is given in the subsection titled "Environmental Problems." Moreover, we show (in the subsection on the characterization of cascade processes) that the integral transform theory developed in this article leads to a simple identification method for multiplicative processes from time series, such as those usually encountered in the study of chaotic mixing processes. Finally, a brief digression on the applicability of the integral transform theory to address mathematical physical problems with boundary conditions of AES type is developed in the section on elliptic equations.

AES Distributions and IFS Theory

We shall consider distribution functions defined on the one-dimensional line. Let $\rho(x)$ be a probability density func-

tion and $\mu(x) = \mu([0, x])$ the corresponding measure (distribution function) whose support is the compact set \mathcal{C} . The support \mathcal{C} can be a finite interval or a Cantor set (Falconer, 1990) as shown in Figure 2b. In any case, the set \mathcal{C} possesses the cardinality of continuum.

A measure (distribution) μ is AES if its derivative does not exist at almost every point of the support \mathcal{C} .

This means that the set of points $\{\xi\}$ for which $\lim_{x \rightarrow \xi^-} \mu(x) \neq \lim_{x \rightarrow \xi^+} \mu(x)$ possesses the cardinality of continuum.

The preceding definition covers the case of distributions defined over Cantor sets and multifractal distributions defined over an interval.

The term *multifractal measure* indicates the sets of distributions that are characterized by a continuous spectrum of Hölder (singularity) exponents α . We shall use $\mu(x; \epsilon)$ to indicate the measure of an interval of width ϵ centered at the point x . The singularity exponent α is defined by the relation

$$\mu(x; \epsilon) \sim \epsilon^\alpha, \quad (2)$$

in the limit of $\epsilon \rightarrow 0$. The scaling properties of multifractal distributions are briefly reviewed in Appendix 1.

In the case of AES distributions, $\rho(x)$ is used to indicate the corresponding density function, $d\mu(x) = \rho(x)dx$. This notation is purely formal since $\rho(x)$ can be regarded as an uncountable superposition of Dirac's delta functions and strictly speaking its mathematical definition is ambiguous. (The reason for this mathematical ambiguity is that for AES distribution an invariant density does not exist. In other terms, the density depends on the lengthscale of observation or, as in the case of IFSP, on the iteration. Nevertheless, keeping this observation in mind, it is fairly customary to plot the density $\rho(x)$ in order to get a direct visual representation of the heterogeneity of AES singular distributions.)

In the development of the theory, however, the definition of density functions is irrelevant since all the quantities of interest are integral quantities, which exist and are mathematically well-posed, averaged over the measure μ (see Eqs. 8–9 below).

One of the most convenient ways to approach AES distributions in a rigorous mathematical way conducive to further applications is by means of the theory of iterated function systems (IFS) (Barnsley, 1988; Forte and Vrscay, 1994).

As IFS with Probability (IFSP) is a system $\{w_h(x), p_h\}_{h=1}^N$ of N contractive maps on a metric space (corresponding in this article to the one-dimensional line) equipped with a system of probability weights p_h , $\sum_{h=1}^N p_h = 1$.

Throughout this article, attention is focused on affine IFSP, for which the transformations $w_h(x)$ are given by

$$w_h(x) = a_h x + b_h, \quad (3)$$

with $|a_h| < 1$, for which a fairly complete theory can be developed.

Computationally, an IFSP system is equivalent to a probabilistic discrete dynamical system, $x_{n+1} = w_h(x_n)$ Prob. p_h , for which, at each iteration n , one of the N transformations $w_h(x)$ is chosen with probability p_h to map x_n into x_{n+1} .

The limit set (attractor) \mathcal{C} of the IFSP, on which the measure is concentrated, satisfies the Hutchinson equation (Barnsley, 1988)

$$\mathcal{C} = \bigcup_{h=1}^N w_h(\mathcal{C}), \quad (4)$$

and the invariant measure μ , the Markov equation (Barnsley, 1988)

$$\mu(\mathcal{A}) = \sum_{h=1}^N p_h \mu(w_h(\mathcal{A})), \quad (5)$$

where \mathcal{A} is an arbitrary measurable set on the one-dimensional line (e.g., an interval or a union of intervals).

It is important to stress that this article is not concerned with the properties of IFSP, which is simply used as a tool to generate and to drive mathematical properties of AES distributions (obtained as invariant measures of an IFSP), which it would otherwise prove difficult to approach.

It should also be pointed out that AES distributions associated with affine IFSP do not cover all the possible multifractal distributions, but represent a specific—albeit extremely useful—case known as *multinomial measure*. This class of measures does, however, represent a fairly satisfactory starting point with a view to highlighting the peculiar properties of AES distributions in chemical engineering applications.

The theory developed in this article holds for invariant measures associated with generic N -map linear IFSP. However, we will refer in most of the examples to two families of distributions associated with 2-map IFSP: (model I) $w_1(x) = x/2$, $w_2(x) = (x+1)/2$, with $p_1 = p$, $p_2 = 1-p$; (model II) $w_1(x) = x/3$, $w_2(x) = (x+2)/3$, with $p_1 = p$, $p_2 = 1-p$, in which p is taken as the parameter characterizing the distribution. The first IFSP gives rise to an invariant measure defined on the unit interval, that is, $\mathcal{C} = [0, 1]$. The uniform density $\rho(x) = 1$ is obtained for $p = 1/2$. Values of p different from $1/2$ give rise to AES distributions (binomial measure). Figure 2A, 2B shows the representation of the invariant densities obtained from model I for $p = 0.3$ and $p = 0.6$, respectively. This family of distributions obviously admits the symmetry $\rho(x) \rightarrow \rho(1-x)$ for $p \rightarrow 1-p$.

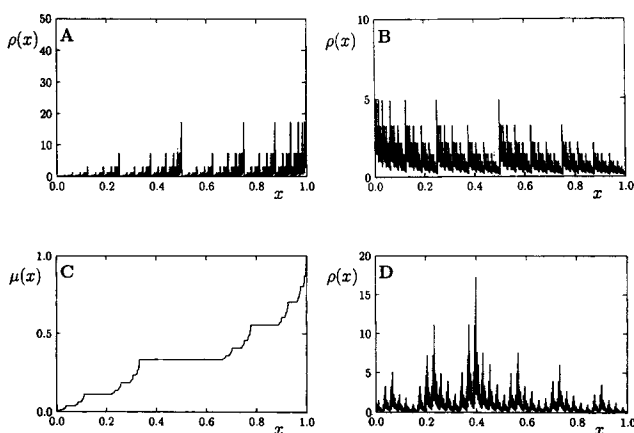


Figure 2. Examples of AES (multifractal) distributions obtained as invariant measures of affine IFSP.

(A) Two-map IFSP (model I) on $\mathcal{C} = [0, 1]$ for $p = 0.3$; (B) 2-map IFSP (model I) for $p = 0.6$; (C) $\mu(x)$ for the 2-map IFSP (model II) generating a multifractal measure on the Cantor middle-third set for $p = 1/3$; (D) 6-map IFSP discussed in the second section, $\mathcal{C} = [0, 1]$.

In the case of model II, the support \mathcal{C} of the measure is the Cantor middle third set, the Hausdorff dimension of which is $d_H = \log 2 / \log 3$.

For $p = 1/2$ a uniform Hausdorff measure is obtained (we agree to call a measure uniform, although defined on a fractal support \mathcal{C} , if the spectrum of its generalized dimensions $D(q)$ is constant, i.e., $D(q) = d_H, \forall q \in (-\infty, \infty)$, where d_H is the Hausdorff dimension of \mathcal{C}), while for $p \neq 1/2$ the corresponding invariant measure displays multifractal features (Figure 2C).

Figure 2D shows another example of AES density obtained from the 6-map IFSP, $w_h(x) = (x + h - 1)/N, h = 1, \dots, 6 = N$, and for a nonuniform configuration of probabilities p_h .

The highly heterogeneous structure of AES distributions is clearly evident in these figure parts. Nevertheless, all the AES distributions depicted in Figure 2 look too "artificial," too regular in their singularity structure, as compared with singular distributions observed in nature. The reason for this apparent regularity is that the corresponding IFSP generating them are constituted by a very few (two) maps and/or possess the same scaling factors a_h , as in the case of the 6-map IFSP in Figure 2D. If one considers slightly more elaborate IFSP in the presence of unequal scaling factors, the resulting invariant measures completely lose any kind of regularity. An example is depicted in Figure 3, deriving from a 6-map IFSP with nonconstant a_h . This distribution looks much closer to some singular chromatograms (a discussion on this apparently naive observation is further developed in the subsection on environmental problems).

From an inspection of Figure 3, one could argue that the resulting distribution consists of well-defined isolated peaks in the presence of some level of "noise" and is therefore discrete in its nature. But all that glitters is not gold. As will become clearer in the next section, the qualitative scaling properties of the integral transforms of $\mu(x)$ are not related to the main peaks, possessing higher probability, but rather to the small probability distribution close to $x = 0$. The fact that the main scaling properties are controlled by extremely low probability events is not a great surprise. The same phenomenon occurs, for example, in the study of chaotic mixing, in which low probability tails possessing high stretching exponents play the leading role in the evolution of material interfaces (Liu et al., 1994; Beigie et al., 1994). Indeed, this analogy is not at all fortuitous, since there are close connections

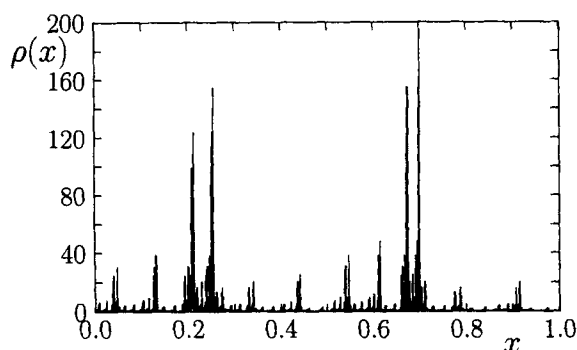


Figure 3. $\rho(x)$ vs. x for a 6-map IFSP with unequal scaling factors a_h , filling the unit interval, that is, $\mathcal{C} = [0, 1]$.

between AES distributions and chaotic mixing processes (see the subsection titled "Reaction in Chaotic Mixing Systems").

One of the most important properties of invariant measures associated with IFSP, and one that makes them particularly suitable for physical mathematical applications, is a theorem for the average of continuous functions with respect to invariant measures of IFSP.

Given an arbitrary continuous function $f(x)$, the average of f with respect to the probability measure μ is defined as

$$\langle f(x) \rangle = \int_{\mathcal{C}} f(x) d\mu(x). \quad (6)$$

The average $\langle f(x) \rangle$ of any continuous function $f(x)$ with respect to the invariant measure associated with an IFSP satisfies the equation (Barnsley, 1988)

$$\begin{aligned} \langle f(x) \rangle &= \int_{\mathcal{C}} f(x) d\mu(x) \\ &= \sum_{h=1}^N p_h \int_{\mathcal{C}} f[w_h(x)] d\mu(x) \\ &= \sum_{h=1}^N p_h \langle f[w_h(x)] \rangle. \end{aligned} \quad (7)$$

Equation 7 is the fundamental relation for further developments and applications to kinetic models involving continuous mixtures.

Closed-form Expression for Integral Transforms

In the perspective of application to continuous kinetic modeling, it is worth analyzing some integral transforms associated with AES distributions.

Attention is focused throughout this article on AES distributions defined on a compact support $\mathcal{C} \subset [0, \infty]$. This is because we are interested in distributions associated with physical properties that are strictly positive (such as rate constants and diffusivities). Without loss of generality, it can be assumed upon normalization that $\mathcal{C} \subset [0, 1]$. Moreover, the maps $w_h(x)$ permit an ordering such that $b_h \leq b_{h+1}$ for $h = 1, \dots, N - 1$. Let us assume that $b_1 = 0$ and $a_h > 0$.

As pointed out by Aris (1991), the theory of chemical reactions involving continuous mixtures is closely connected with the theory of integral transforms of distributions.

More specifically, let us define the Laplace transform of a normalized measure, whose support is \mathcal{C} , as

$$\mathcal{L}(s) = \int_{\mathcal{C}} \exp(-sx) d\mu(x), \quad (8)$$

and the Stieltjes transform as

$$\mathcal{S}(z) = \int_{\mathcal{C}} \frac{d\mu(x)}{1 + zx}. \quad (9)$$

Equation 7 can be applied to obtain a closed-form expression for these integral transforms of invariant measures associated with IFSP.

In the case of $f(x) = \exp(-sx)$, from Eq. 7 it follows that

$$\begin{aligned} \int_{\mathbb{C}} \exp(-sx) d\mu(x) &= \sum_{h=1}^N p_h \int_{\mathbb{C}} \exp[-s(a_h x + b_h)] d\mu(x) \\ &= \sum_{h=1}^N p_h \exp(-sb_h) \int_{\mathbb{C}} \exp(-a_h sx) d\mu, \quad (10) \end{aligned}$$

that is,

$$\mathcal{L}(s) = \sum_{h=1}^N p_h \exp(-sb_h) \mathcal{L}(a_h s). \quad (11)$$

Analogously, in the case of the Stieltjes transform, by plugging $f(x) = (1+xz)^{-1}$ into Eq. 7, it follows that

$$\mathcal{S}(z) = \sum_{h=1}^N \frac{p_h}{1+b_h z} \mathcal{S}\left(\frac{a_h z}{1+b_h z}\right). \quad (12)$$

Equations 11–12 are the functional equations expressing the Laplace and Stieltjes transforms of invariant measures associated with a generic affine IFSP.

It is convenient to draw a distinction between distributions generated by unimodular and by nonunimodular IFSP.

An affine IFSP is said to be *unimodular* if all the transformations $w_h(x)$ admit the same scaling factor, that is, $a_h = a$, $h = 1, \dots, N$. In the one-dimensional case, the class of unimodular IFSP coincides with that of similar IFSP.

For unimodular IFSP, the Laplace transform of AES invariant measures can be expressed in closed form as a convergent infinite product (see Appendix 2):

$$\mathcal{L}(s) = \prod_{n=0}^{\infty} \left[\sum_{h=1}^N p_h \exp(-a^n b_h s) \right], \quad (13)$$

where $\mathcal{L}(s)$ is analytic in the half-plane $\text{Re}[s] > 0$. Moreover, the sequence of approximants $\{L_n(s)\}$

$$L_n(s) = \prod_{k=0}^n \left[\sum_{h=1}^N p_h \exp(-a^k b_h s) \right], \quad (14)$$

converges uniformly toward $\mathcal{L}(s)$ (see Appendix 2). This result is of the utmost importance in practical computations.

In the case of nonunimodular IFSP, the Laplace transform of the corresponding AES invariant measure can be computed from the recursion scheme

$$L_{n+1}(s) = \sum_{h=1}^N p_h \exp(-sb_h) L_n(a_h s), \quad L_0(s) = 1, \quad (15)$$

since the sequence $\{L_n(s)\}$ obtained through Eq. 15 is uniformly convergent toward $\mathcal{L}(s)$. Analogous results can be obtained for the Fourier transform $\Phi(\omega)$, ω real, defined as

$$\Phi(\omega) = \int_{\mathbb{C}} \exp(I\omega x) d\mu(x), \quad (16)$$

where $I = \sqrt{-1}$, by replacing $-s$ with $I\omega$ in the expressions for the Laplace transforms, Eqs. 13–15. Fourier transforms are applied in the section on elliptic equations.

The latter approach can also be applied to the case of Stieltjes transforms $\mathcal{S}(z)$, expressed by the functional Eq. 12: $\mathcal{S}(z)$ can be obtained as the limit of the recursive process

$$S_{n+1}(z) = \sum_{h=1}^N \frac{p_h}{1+b_h z} S_n\left(\frac{a_h z}{1+b_h z}\right) \quad S_0(z) = 1, \quad (17)$$

since the sequence $\{S_n(z)\}$ converges uniformly toward $\mathcal{S}(z)$.

The uniform convergence of the sequences $\{L_n(s)\}$, $\{S_n(z)\}$ makes the computation of the Laplace and Stieltjes transforms easy and arbitrarily accurate.

Another important property of integral transforms of AES distributions is their scaling behavior with respect to the argument.

The Laplace transform $\mathcal{L}(s)$ behaves asymptotically (i.e., for large s) as (see Appendix 2)

$$\mathcal{L}(s) \sim s^{-\beta}, \quad (18)$$

where the exponent β is given by

$$\beta = \frac{\log p_1}{\log a_1}. \quad (19)$$

The scaling behavior of the Stieltjes transform is particularly interesting. By assuming a power-law scaling for large z , $\mathcal{S}(z) = Az^{-\gamma} + o(z^{-\gamma})$, from Eq. 12 it follows that

$$Az^{-\gamma} = Ap_1 a_1^{-\gamma} z^{-\gamma} + B/z + o(z^{-\gamma}), \quad (20)$$

where A and B are two constants.

Two situations may occur. If $\gamma < 1$, the first term on the righthand side of Eq. 20 controls the asymptotic behavior. Therefore, $1 = p_1 a_1^{-\gamma}$, which implies

$$\gamma = \frac{\log p_1}{\log a_1}. \quad (21)$$

This occurs for values of $p_1 > a_1$. For values of $p_1 < a_1$, the second term on the righthand side of Eq. 20 controls for large z , and therefore

$$\gamma = 1. \quad (22)$$

This result can be expressed in a compact form as $\gamma = \min\{1, \log p_1 / \log a_1\}$.

This means that the Stieltjes transform of a family of AES distributions parametrized with respect to the probability weights $\{p_h\}$ exhibit a phase transition in the asymptotic behavior

$$\mathcal{S}(z) \sim \begin{cases} 1/z & \text{for } p_1 < p_c \\ 1/z^\gamma & \text{for } p_1 > p_c, \end{cases} \quad (23)$$

where the critical value is $p_c = a_1$.

This result is also shared by continuous distributions (Ho, 1996). To conclude, let us analyze the behavior of the Stieltjes transform at the critical point $p_1 = p_c$. At $p = p_c$, $\mathcal{S}(z)$ exhibits a weak logarithmic dependence in the prefactor of the $1/z$ scaling. For example, in the case of a uniform distribution on $[0, 1]$, it follows readily that $\mathcal{S}(z) = \log(1+z)/z$. Similar behavior is observed in the other cases. In the case of the IFSP generating the Cantor middle third set (model II), the analysis of the Stieltjes transform reveals that at $p = p_c = 1/3$, $\mathcal{S}(z) = A \log(1+z)/z$, where the constant A is bounded between 0.60 and 0.64.

Application to Models of Continuous Kinetics

This section applies the results derived in the preceding section to models of continuous kinetics.

The main purpose of this section is to show that it is possible to subject almost-singular distributions in kinetic applications to rigorous treatment by applying the methods just developed. In particular, it is interesting to observe that AES distributions can be qualitatively regarded as a very interesting case of the “almost discrete” distributions discussed by Aris (1994), which are characterized by the fact that the distribution is singular at almost every point belonging to the support \mathcal{C} , but with the property that each point of \mathcal{C} is an accumulation point of points belonging to \mathcal{C} .

The analysis is developed systematically by considering classic schemes of continuous lumping developed for smooth, regular distributions by Ho and Aris (1987), Astarita and Ocone (1988), Astarita (1989), Aris (1989), Astarita and Nigam (1989), and Chou and Ho (1988, 1989).

Throughout this section it is assumed that the mixture is parametrized continuously with respect to a characteristic kinetic rate k . Given the assumption that k is defined on a compact (bounded) support $k \in [0, k_{\max}]$, it is convenient to define the dimensionless parameter $x = k/k_{\max} \in [0, 1]$. We consider initial (in batch processes) or inlet \mathcal{A} (in flow systems) distributions parametrized with respect to x . For the sake of mathematical convenience, these distributions are taken within the subclass of AES distributions that can be generated as invariant measures of affine IFSP. This is not a severe limitation in the analysis in view of the fact that we are interested in the qualitative features peculiar to AES distributions, and that any other distribution can be approximated by members of this class (Barnsley, 1988).

Linear and nonlinear batch reactions

We first consider the simplest case of a linear batch reaction in a continuous mixture. Let $c(x, t)$ be the concentration distribution parametrized with respect to the dimensionless kinetic rate x defined on the compact support \mathcal{C} , and let the initial distribution be $c(x, 0) = c_o(x) = c_o \rho(x)$, with $\int_{\mathcal{C}} \rho(x) dx = \int_{\mathcal{C}} d\mu(x) = 1$.

In this case, the balance equation is simply given by

$$\frac{\partial u(x, \theta)}{\partial \theta} = -xu(x, \theta), \quad (24)$$

where $\theta = tk_{\max}$ and $u(x, \theta) = c(x, \theta)/c_o$. The solution of Eq. 24 is readily obtained as $u(x, \theta) = \rho(x)\exp(-x\theta)$. The total

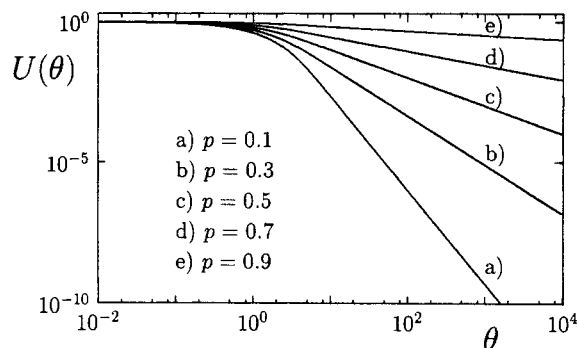


Figure 4. $U(\theta)$ vs. θ for a linear batch kinetics.

The initial distribution is obtained from model I for different values of the parameter p controlling the shape of the distribution.

normalized concentration $U(\theta) = \int_{\mathcal{C}} u(x, \theta) dx$ is therefore the Laplace transform of the initial distribution, Eq. 8.

$$U(\theta) = \mathcal{L}(\theta), \quad (25)$$

which is expressed in closed form for AES distributions in the previous section, Eq. 13. As an example, let us consider the binomial measure $\mu(x)$, $d\mu(x) = \rho(x) dx$, generated by the 2-map IFSP, model I, discussed in the second section, with p as a parameter controlling the structure of the distribution.

Figure 4 shows the behavior of $U(\theta)$ vs. θ in this case for different values of p . From Eq. 25, the asymptotic scaling predicted by Eq. 18 is simply $U(\theta) \sim \theta^{-\beta}$. This result also holds for smooth distributions (Ho and Aris, 1987).

The case of nonlinear uniform kinetics can be treated in exactly the same way. To simplify the notation, we consider the following scheme of uniform kinetics:

$$\frac{\partial c(k, t)}{\partial t} = -kc(k, t)\mathfrak{F}[\int c(k, t) dk], \quad (26)$$

where $\mathfrak{F}[y] = Ay^{n-1}$ is a dimensionless functional expressing an n -order reaction. In dimensionless form, Eq. (26) becomes

$$\frac{\partial u(x, \theta)}{\partial \theta} = -xu(x, \theta)\Lambda U^{n-1}(\theta), \quad (27)$$

where $\Lambda = A(k_{\max}c_o)^{n-1}$. By applying the approach for nonlinear uniform kinetics developed by Astarita and Ocone (1988), and by putting $H(s) = \mathcal{L}(s)$ for the Laplace transform of the initial distribution, it follows that

$$U(\theta) = H\left(\Lambda \int_0^\theta U^{n-1}(\xi) d\xi\right), \quad (28)$$

which can be rewritten in the form

$$\frac{dU(\theta)}{d\theta} = \Lambda U^{n-1}(\theta) \frac{dH(y)}{dy} \Big|_{y=H^{-1}[U(\theta)]}. \quad (29)$$

In the limit of large θ , $U(\theta)$ tends to zero, and by recalling Eq. 18, it follows that $dH(y)/d(y)|_{y=H^{-1}(U)} \sim -U^{(\beta+1)/\beta}$. The apparent order of reaction ν , $dU/d\theta \sim -U^\nu$ is therefore given by

$$\nu = \frac{\beta n + 1}{\beta}. \quad (30)$$

This result is analogous to that derived by Astarita (1989) in the case of smooth (gamma) initial distributions (see Ho, 1996, for details). We may therefore conclude that both smooth and AES distributions qualitatively display the same asymptotic features in the case of batch reactions.

Reactions in a CSTR

Let us now examine the case of steady-state kinetics in a CSTR, which has been considered by Astarita and Nigam (1989) and by Aris (1991). Astarita and Nigam have shown for first-order reactions that, independently of the nature of the (smooth) distribution function, and provided that $\rho(x)$ is nonsingular at $x = 0$, the dimensionless lumped concentration $U = \int c(x) dx / c_0$ scales for high residence times τ as $U \sim 1/\tau$.

In the case of AES inlet distributions, a rather interesting phenomenon occurs. From the balance equation at steady state, it readily follows that $u(x) = \rho(x)/(1 + Tx)$, where $T = \tau k_{\max}$ is the dimensionless residence time, and therefore

$$U(T) = \int_0^1 \frac{\rho(x) dx}{1 + Tx} = \int_0^1 \frac{d\mu(x)}{1 + Tx} = \mathcal{S}(T), \quad (31)$$

that is, the normalized lumped concentration $U(T)$ is the Stieltjes transform of the feed distribution evaluated at T . The theory of Stieltjes transforms developed earlier for AES distributions can therefore be applied.

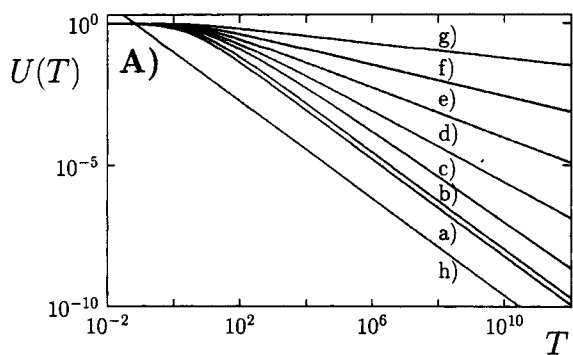
Let us consider the behavior of the lumped concentration $U(T)$ vs. T for a family of AES distributions. Figures 5A–5B show $U(T)$ vs. T for the two families of AES distributions (models I and II, i.e., binomial measures on the unit interval and on a Cantor set).

As can be observed, there is a sudden change (analogous to a phase transition) in the asymptotic slope, as predicted by Eq. 23,

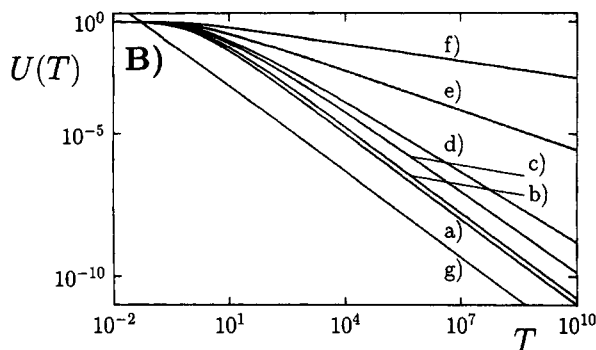
$$U(T) \sim \begin{cases} T^{-1} & \text{for } p < p_c \\ T^{-1} \log(1 + T) & \text{for } p = p_c \\ T^{-\gamma} & \text{with } \gamma < 1 \text{ for } p > p_c. \end{cases} \quad (32)$$

Indeed, this qualitative feature of $U(T)$ resembling a phase transition cannot occur for atomic distributions formed by a finite number of Dirac's delta terms, but may arise in connection with smooth distributions displaying a singularity at $x = 0$ (Ho, 1996).

However, AES and smooth distributions display different behavior for small T . In the case of AES distributions, $U(T)$ is practically equal to 1, that is, admits extremely low conversions, for $T < 1$. This is a consequence of the fact that $x = 0$ is an accumulation point of singularities.



(a)



(b)

Figure 5. $U(T)$ vs. the dimensionless residence time T for linear continuous kinetics in a CSTR, for different values of the parameter p controlling the distribution.

(A) Model I, distribution on the unit interval: (a) $p = 0.01$; (b) $p = 0.3$; (c) $p = p_c = 1/2$; (d) $p = 0.6$; (e) $p = 0.7$; (f) $p = 0.8$; (g) $p = 0.9$; (h) $U(T) \sim T^{-1}$. (B) Model II distribution on the Cantor middle-third set: (a) $p = 0.1$; (b) $p = 0.2$; (c) $p = p_c = 1/3$; (d) $p = 0.4$; (e) $p = 0.6$; (f) $p = 0.8$; (g) $U(T) \sim T^{-1}$. The transition is evident in the slope (on a log-log plot) of these curves occurring at $p = p_c$. $p_c = 1/2$ for model I; $p_c = 1/3$ for model II.

The behavior of $U(T)$ for small values of T is related to the moment hierarchy $\{m_n\}$,

$$m_n = \int_0^1 x^n p(x) dx = \int_0^1 x^n d\mu(x), \quad (33)$$

since the normalized lumped concentration $U(T)$ can be regarded as a moment-generating function associated with the feed distribution,

$$m_n = \frac{(-1)^n}{n!} \left. \frac{d^n U(T)}{dT^n} \right|_{T=0}. \quad (34)$$

In the case of AES distributions, the moment hierarchy $\{m_n\}$ scales with n as $m_n \sim n^{-\zeta}$, where the exponent $\zeta = \log p_N / \log a_N$ (Giona, 1995). This power-law scaling of the moment hierarchy with n is a peculiar property of the continuous singularity structure displayed by AES distributions.

The analysis of nonlinear uniform kinetics is completely analogous, and is reported for the sake of completeness, con-

sidering the same class of uniform kinetics analyzed for batch processes,

$$\frac{c_o(k) - c(k)}{\tau} = kc(k) \mathfrak{F}[\int c(k) dk]. \quad (35)$$

Upon normalization, and after some algebra, one obtains for the lumped concentration U the expression

$$U = \mathfrak{S}[TAU^{n-1}], \quad (36)$$

where $\mathfrak{S}(z)$ is, as before, the Stieltjes transform of the inlet concentration. Therefore, for high dimensionless residence times T , the scaling of U with respect of T is given by

$$U \sim T^{-\gamma/(1+\gamma(n-1))}, \quad (37)$$

which should be compared with the scaling $U(T) \sim T^{-1/n}$ occurring for the class of smooth distributions considered by Astarita and Nigam (1989).

The results obtained for batch reactions can be extended in a straightforward way to the steady-state behavior of a plug-flow reactor (PFR) by replacing the dimensionless time θ with the dimensionless residence time T . Therefore, from Eq. 31 (for $n = 1$, i.e., first-order reaction) it follows that the apparent reaction order in a PFR is given by $\nu_{\text{PFR}} = (1 + \beta)/\beta$, and for a CSTR, Eq. 37, $\nu_{\text{CSTR}} = 1/\gamma$. Since from Eqs. 21–22, we have $\gamma = \min\{1, \beta\}$, it follows that $\nu_{\text{PFR}} > \nu_{\text{CSTR}}$. This result is analogous to the finding of Ho (1996) in the case of smooth distributions (see Figure 6 of Ho's article).

An important practical issue in order to apply AES singular distributions to complex mixtures lies in the estimation of parameters a_h , p_h directly from the initial distribution. Indeed these parameters, and a_1 , p_1 in particular, enter in the expressions for the exponents γ , β and for the critical threshold p_c , which characterize the asymptotic properties of the global conversion for large residence times. The answer to this problem depends on the quality of the data for the initial distribution, since as discussed in the second section, multifractal measures are intrinsically sensitive to the length-scale, that is, to the resolution. A method to derive a_h and p_h characterizing the initial (inlet) distribution makes use of the scaling properties expressed by means of the multifractal spectrum $f(\alpha)$ (Appendix 1). This method is discussed by Vojak et al. (1994), by Vojak (1996), and by Levy-Vehel (1996). Another approach is based on the moment analysis of the initial distribution (Abenda and Turchetti, 1989; Bessis and Demko, 1991). In the case where accurate data sets for the initial distribution are available, it is possible to develop efficient identification algorithms just by exploiting the scaling properties of integral transforms, as is discussed in the subsection on the characterization of cascade processes. Since the method outlined in that subsection is new, no comparisons with other identification methods are available. The detailed algorithmic and numerical analysis of this method lies outside the aim of this article and will be developed elsewhere.

To complete the analysis, let us briefly consider the transient dynamics, with analysis limited to the linear case in order to simplify the notation. The solution of the transient

response with vanishing initial condition can be expressed by the equation

$$U(\theta) = \int_{\mathbb{C}} u(x, \theta) dx = \int_{\mathbb{C}} \frac{d\mu(x)}{1 + Tx} [1 - \exp(-\theta/T - x\theta)] \\ = \mathfrak{S}(T) - \exp(-\theta/T) \mathfrak{M}(\theta, T), \quad (38)$$

where $\theta = tk_{\text{max}}$ and $\mathfrak{M}(\theta, T) = \int_{\mathbb{C}} \exp(-x\theta) d\mu(x)/(1 + Tx)$ indicates an integral transform of the feed distribution that we can conventionally label as a *mixed Laplace–Stieltjes* transform. This name comes from the observation that $\mathfrak{M}(0, T) = \mathfrak{S}(T)$ and $\mathfrak{M}(\theta, 0) = \mathfrak{L}(\theta)$.

For the mixed Laplace–Stieltjes transform of distributions generated by means of affine IFSP, the following functional relation holds:

$$\mathfrak{M}(\theta, T) = \sum_{h=1}^N \frac{p_h \exp(1 - b_h \theta)}{1 + b_h T} \mathfrak{M}\left(a_h \theta, \frac{a_h T}{1 + b_h T}\right), \quad (39)$$

which is analogous to Eqs. 11–12.

All the approximation methods discussed in the third section for the Laplace and Stieltjes transforms can therefore be applied to $\mathfrak{M}(\theta, T)$.

Practical Application of the Theory

An important issue that should be addressed is the practical impact of the theory developed in engineering applications, that is, whether (1) AES distributions and (2) the integral transform theory of AES distributions can be applied to address, and hopefully solve, real physical problems of chemical engineering interest.

Before developing this issue, by showing a few examples, it is worthwhile to bear in mind that any mathematical modeling intrinsically implies some level of approximation of the physical reality. A model can be considered satisfactory and interesting to study if the approximations introduced admit a physical origin, simplify the mathematical analysis of the problem, and enable us to extend our range of investigations into more complex and/or new fields.

This section attempts to give an answer as regards the usefulness of the description of complex mixtures by means of AES distributions, their physical origin in some (indeed fairly common) fluid-dynamic applications, and the application of the integral transform theory to approach the identification problem of AES distributions.

The topics covered in the following four sections admit this as the only common denominator. Otherwise, the physical phenomenologies (which range from pollutant distributions to chaotic mixing, from vehicular flows to experimental data analysis) are not strictly related to each other. We apologize for the sudden changes in the physical phenomenologies treated in these subsections, which are motivated by the aim of presenting a broad range of applications of AES distributions to experimental and engineering problems.

Environmental problems

In chemical kinetics it is rather difficult to find unquestionable and already known examples of chemical mixtures that

cannot be described with acceptable accuracy either by means of discrete lumping or through smooth continuous distributions. For example, the diesel-fuel mixture analyzed by Moore and Anthony (1989) is a typical example in which the continuous approach fails but discrete lumping is still acceptable if one overlooks the composition fluctuations around each main peak.

However, in many environmental problems involving pollutant distributions, the situation is much more complex. The level of heterogeneity in mixture composition can be so intrinsic that both discrete and/or continuous lumping do not seem the best possible description. A typical example has recently been shown by Zou et al. (1996) in the experimental analysis of the distribution of organic contaminants in two lakes (Lake Taihu and Lake Wuliku, China). The experimental analysis was performed by means of gas chromatography. Water samples were first pretreated in order to remove suspended solids by means of a separation process involving a packed bed filled with resin (see Zhou et al., 1996, for details). The adsorbed contaminants were then extracted and passed through an evaporator. The results of gas chromatographic analysis (see figure 2 of Zou et al., especially the data for Lake Wuliku) show an extremely heterogeneous pattern with distributed peaks and many singularities. (It should be mentioned that the three principal peaks shown in figure 2 of Zhou et al. refer to internal calibration standards, and not to the contaminant distribution.)

The authors found more than 800 different organic components (but as they said, this is only a preliminary chemical characterization, and the mixture is indeed much more complex), which could be roughly grouped into 80 principal components. These chromatographic data are a typical example of a mixture for which both discrete and smooth continuous approaches are not adequate, and the best global characterization is probably given by the application of AES distributions, by taking as a characteristic parameter (label) the retention time or equivalently the adsorption constant.

This example indicates that AES distributions may find a virgin field of application (with important practical consequences) in many other environmental issues connected with the study of pollutant distributions. The AES nature of a mixture modifies the development of optimal adsorption units for separation and purification of complex mixtures discussed, for example, by Sheintuch and Rebhun (1988) and by Annesini et al. (1994).

It is important to stress that the methodologies developed in signal processing for characterizing multifractal measures (see the subsection on characterizing cascade processes) may be directly used to extract from the experimental data (e.g., chromatograms) the characteristic parameters of the corresponding AES distribution.

Reaction in chaotic mixing systems

The preceding subsection discussed an experimental observation of a highly singular pollutant distribution in which the application of the AES-distribution theory is advisable in order to design efficient separation units, for example, by means of adsorption-based processes.

In this subsection we analyze another experimental confirmation, namely chaotic mixing processes with reaction, which

is of a more fundamental nature, highlighting the physical origin of AES distributions. The discussion developed is mostly qualitative and is grounded on known results.

It is known, after almost two decades of research, that mixing processes at low Reynolds numbers show chaotic features (Ottino, 1989; Wiggins, 1992). Chaotic mixing has been observed in stirred tanks, static mixers, and cavity (periodic and aperiodic) flows. Some universal features characterize chaotic mixing as a consequence of the "stretching and folding" of material elements.

A vast literature on experimental, simulation, and theoretical results has analyzed the statistical characterization of chaotic mixing systems, focusing on the statistics of stretching exponents and of the curvature of material lines (Muzzio et al. 1992a,b; Liu et al., 1994; Beigie et al., 1994; Pentek et al., 1995; Liu and Muzzio, 1996).

All the published results have clearly shown the presence of highly singular spatial distributions in all the physical observables related to the process (such as stretching exponents and curvature), which can be modeled macroscopically by means of multiplicative processes (Beigie et al., 1994).

A critical review of the literature in the field, oriented toward the purposes of this article, leads us to point out the following main issues that are nowadays widely accepted and experimentally confirmed. (1) The spatial structure of the stretching field possesses multifractal features. This has been shown by Muzzio et al. (1992a,b) and by Pentek et al. (1995). The highly singular spatial structure of the stretching field is clearly depicted by Liu et al. (1994) for cavity flow. (2) The functional form of the distribution function $H_n(\lambda)$ of the stretching exponent λ at iteration n (n is the dimensionless time in a Poincaré stroboscopic map) indicates that these distributions cannot be associated with a multiplicative process generating uniform (smooth) spatial distributions (e.g., Beigie et al., 1994). (3) The singular distribution of all physical observables (stretching exponents, curvatures) maps onto a corresponding highly singular structure of the striations (of material elements), as observed experimentally in cavity flow systems. The results shown by Pentek et al. (1995) for the leapfrogging vortex-pair dynamics indicate the multifractal nature of striations (see in particular figure 14 of the article by Pentek et al.), and its implications on transport and kinetics are evident. In order to describe this phenomenon in reacting systems, lamellar models of reacting/diffusing systems have been developed by Muzzio and Ottino (1989a,b). For high kinetic rates compared with diffusional rates, the spatial local structure of the striations is the main element responsible for the temporal behavior of the overall kinetics.

Let us connect all these observations with the AES theory developed in previous sections, that is, in terms of continuous kinetic modeling. In the study of mass transfer let us consider a lamellar model, and analyze it in terms of a cell description. Each striation is regarded as a cell in which the concentration of reactants is uniform. Under this assumption, the corresponding balance equations for a one-dimensional lamellar model are given by

$$\frac{dc_i^\alpha}{dt} = \frac{1}{\tau_{i+1}} (c_{i+1} - c_i) + \frac{1}{\tau_{i-1}} (c_{i-1} - c_i) + r(c_i^1, \dots, c_i^S), \quad (40)$$

where c_i^α is the concentration of the α th species in the i th cell (lamella); r the reaction rate; S the total number of species; and τ_i the retention time of the i th lamella, which is roughly proportional to the local striation thickness.

If we assume a continuum description of the mixture, it is natural to take τ (and ultimately the lamellar thickness) as the parameter (label). This leads to a reaction/diffusion kinetics in the presence of an AES spatial distribution of τ . Of course, this picture is highly idealized. (It should be always borne in mind that the lamellar model discussed by Muzzio and Ottino is also highly idealized, since it corresponds to a quenched analysis of a mixing system.) A more correct description should necessarily take into account the destruction of the lamellae due to reaction, and the corresponding regeneration due to mixing. The assumption of time-independent values of the parameters τ_i may be physically justified only if the interplay between creation (mixing) and annihilation (reaction) of the lamellae will eventually lead to stationary lamellar distributions. (In the articles introducing lamellar models (Muzzio and Ottino, 1989a,b) this phenomenon does not occur since no lamellar creation is allowed, because the system is considered to be quenched.)

In any case, bearing in mind the crude simplifications assumed, this example highlights in a simple and clear way how AES distributions may naturally appear in a realistic description of real chemical processes.

The highly singular spatial of physical observables in chaotic flows corresponds to fairly smooth global distribution functions, that is, the probability $p(\lambda)d\lambda$ of finding a value of an observable Λ between λ and $\lambda + d\lambda$ is smooth. This is exactly what happens in the case of AES distributions. Let us give a simple example of this property. Let us take an arbitrary affine IFSP $\{w_h(x) = a_h x + b_h, p_h\}_{h=1}^N$ possessing an AES invariant measure and study the distribution of the contraction factors. In the analogy with mixing problems, the contraction factors can be assumed to be inversely proportional to the stretching exponents. For incompressible two-dimensional flow the product of the eigenvalues is always equal to 1 (area-preserving property). The stretching of $\lambda > 1$ in the unstable direction corresponds to a contraction of $1/\lambda$ along the local stable subspace. At iteration n , the contrac-

tion factor attains the values $\Pi_{h=1}^N a_h^{j_h}$, with $\sum_{h=1}^N j_h = n$, and the statistics of the contraction factors is a multinomial distribution. The probability of finding the value $\lambda = \Pi_{h=1}^N a_h^{j_h}$ for the contraction factor at iteration n is given by $n! / \Pi_{h=1}^N j_h!$. However, the spatial distribution of the contraction factors is highly singular: it is an AES distribution qualitatively similar to those distributions depicted in Figures 1–3.

From the preceding discussion, the physical origin and the potentialities in the application of AES distributions clearly appears beyond any reasonable doubt (unless motivated solely by aprioristic and nonscientific criticism) in modeling reaction/diffusion processes in mixing systems. If we connect the vast research developed in the past with the recent trends in the theory of mixing, it may be argued that the theory of AES distributions will become one of the principal analytical tools in the development of a modern theory of mixing.

To sum up, the intrinsic “stretching and folding dynamics” characterizing chaotic mixing is one of the causes of the occurrence of multiplicative processes, and ultimately of AES distributions in physical systems. A further experimental example of this phenomenon is given in the next subsection, while the final subsection focuses on a practical application of the integral transform theory to extract the characteristic scaling parameters of the multiplicative process directly from the initial distribution functions.

Nonstandard transport phenomena

A rather nonstandard transport problem that recently attracted considerable attention is related to traffic flows (vehicular motion). This problem has a direct practical impact on the solution of many environmental problems, and more or less deeply influences the quality of life in all big cities. Besides this, vehicular flow has significant connections with more classic fluid dynamics (granular flow in particular) and kinetic theory, as witnessed by the monograph published almost two decades ago by Ilya Prigogine (Prigogine and Herman, 1971).

From the macroscopic point of view (i.e., in the continuum approach), there is some experimental evidence that traffic flow can be acceptably described by Burger's equation (see Vojak (1996) and reference therein):

$$\frac{\partial u}{\partial t} + v_{\max} \left(1 - 2 \frac{u}{u_{\max}} \right) \frac{\partial u}{\partial x} = \nu \frac{\partial^2 u}{\partial x^2}, \quad (41)$$

where $u = u(x, t)$ is the vehicular density; t time; x the spatial coordinate in the main traffic direction; and $\nu > 0$ a constant related to a “vehicular viscosity,” v_{\max} , u_{\max} , respectively, the maximum velocity and the maximum admissible density. (The viscous term comes from the assumption, discussed in Vojak (1996), that a driver adapts the velocity not only as a function of the distance separating him from the preceding vehicle but also as a function of the change (gradient) of this distance.)

Due to the intrinsic “granular” nature of vehicular flow, discrete model and direct experimental observations are even more interesting than continuous models. Discrete approaches are the direct counterpart of kinetic theories in classic transport phenomena (Prigogine and Herman, 1971). Experimental observations of traffic flows related the fluctua-

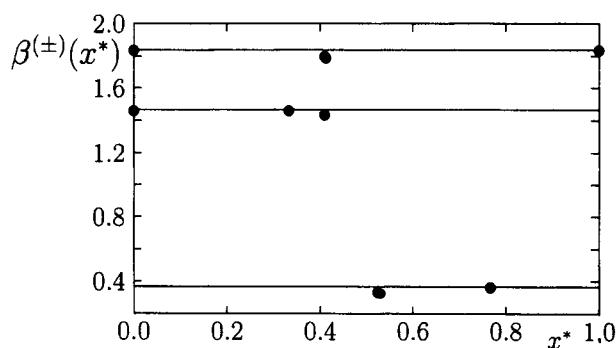


Figure 6. $\beta^{(\pm)}(x^*)$ vs. x^* for several x^* chosen at random.

The data are obtained from the application of the random iteration algorithm to a 3-map IFSP. The three horizontal lines are $\beta_h = \log p_h / \log a_h$, $h = 1, 2, 3$.

tions in the number of vehicles flowing through a given fixed section (Eulerian approach) have recently been reported by Vojak (1996) for several main locations in the city of Paris. Besides some degree of seasonal trend (related to deterministic daily fluctuations in traffic flow), the experimental data show an intrinsic degree of singularity that is characteristic of an underlying multifractal structure (i.e., an AES distribution) in the flow. In particular Vojak (1996) has shown that a multifractal approach to vehicular fluctuations is able to predict the experimental data with accuracy.

Three conclusions may be drawn from this phenomenological result: (1) in vehicular flows the structure of density fluctuations possesses intrinsic features typical of AES distributions; (2) this result can be extended to analogous phenomenologies, such as information flow through computer networks and granular flow; and (3) the physical motivation for the presence of an AES structure in traffic flow is ultimately related to the presence of avalanches and multiplicative cascades (this is the main physical analogy between traffic and granular flows).

Characterization of cascade processes from experimental time series

In the subsection, "Reaction in Chaotic Mixing Systems," we discussed the physical origin of AES distributions in cascade and multiplicative processes associated, for example with mixing problems. This is a basic result underlying the introduction of multifractal formalism in fluid dynamics (especially in turbulence), starting from the pioneering work of Mandelbrot (1974).

Several attempts to model chaotic mixing (distribution of stretching exponents) by means of multinomial processes (a multinomial multiplicative process is equivalent to an affine IFSP of the form $\{a_h x + b_h, p_h\}_{h=1}^N$, considered throughout this article) have been proposed (Beigie et al. (1994) and references therein).

An important practical issue, in order to achieve a fully quantitative description of the underlying AES distributions in all the applications, is to obtain directly from the initial distribution (e.g., in the form of a time series $\{x_i\}_{i=1}^{N_s}$) the characteristic parameters characterizing the distribution itself (such as a_h, p_h).

This problem can be stated as follows: let $\{x_i\}_{i=1}^{N_s}$ be a data set for an observable characteristic of an AES distribution and determine the structure of the underlying multiplicative process. Without loss of generality let us rescale x_i within the unit interval $[0, 1]$, and assume that the limit set on which the measure is concentrated is $[0, 1]$ itself. This occurs in most of the practical applications, although as shown by Pentek et al. (1995) in the case of leapfrogging vortex pair flow, the structure of the evolution of material lines may have strictly fractal properties (i.e., the support is a Cantor dust, i.e., contains holes at all the lengthscales). In modeling chaotic mixing systems, this problem has a real impact, since with present computer resources is it not difficult to obtain extremely large and detailed time series for realistic models of mixing. In these applications, the data set $\{x_i\}$ may be related to the behavior of the curvature, stretching exponents, and so on, on a given cross section of the flow.

Let us suppose that the underlying process can be described by means of a linear multiplicative process (i.e., by

means of an IFSP $w_h(x) = a_h x + b_h$ with probability p_h , $h = 1, \dots, N$).

The integral transform theory discussed in this article furnishes a simple and powerful method to detect the features of the IFSP associated with the data set. Let us consider the Laplace transform. Its scaling behavior for large s , Eqs. 18–19 bring out the scaling properties (exponent β) of the underlying measure μ in the neighborhood of $x = 0$.

In order to obtain information for the scaling behavior in the neighborhood of other points, say $x^* \in [0, 1]$, which are accumulation points of the support of μ , we can define two associated data sets, referred to as the right- and left-shifted data sets, $\{x_i^{(\pm)}(x^*)\}$,

$$x_i^+(x^*) = x_i - x^* \mod 1, \quad x_i^-(x^*) = x^* - x_i \mod 1 \\ i = 1, \dots, N_s. \quad (42)$$

The meaning of this shifting operation is to translate the behavior in the neighborhood of $x = x^*$ into the behavior close to $x^{(\pm)} = 0$, and thus to apply the scaling results already found, Eq. 18.

The Laplace transform of $\{x_i^{(\pm)}(x^*)\}$ can be obtained numerically directly from the shifted data set,

$$\mathcal{L}_{\text{num}}^{(\pm)}(s; x^*) = \frac{1}{N_s} \sum_{i=1}^{N_s} \exp[-s x_i^{(\pm)}(x^*)], \quad (43)$$

where the subscript num stands for "numeric."

According to Eq. 18, the scaling behavior of $\mathcal{L}_{\text{num}}^{(\pm)}(s; x^*)$ vs. s takes the form

$$\mathcal{L}_{\text{num}}^{(\pm)}(s; x^*) \sim s^{-\beta^{(\pm)}(x^*)}, \quad (44)$$

in which the exponent $\beta^{(\pm)}(x^*)$ depends on the position, that is, on x^* .

Under the hypothesis stated previously (i.e., AES generated by means of a linear multiplicative process, linear IFSP), the exponents $\beta^{(\pm)}(x^*)$ will attain N distinct values $\beta_h = \log p_h / \log a_h$, $h = 1, \dots, N$ on a dense subset of \mathcal{C} . In this way, the exponents β_h controlling the scaling properties of AES distributions in continuous kinetic modeling (the fourth section) can be obtained. It is important to stress that the method gives a simple and practical criterion to distinguish between linear and nonlinear multiplicative processes. Moreover, in all the cases in which the values of the probability weights are known from physical reasons, this method makes it possible to determine the values of all the a_h that characterize the process. To give an example, let us consider a time series associated with a 3-map IFSP: $w_1(x) = x/3$, $p_1 = 0.2$, $w_2(x) = x/4 + 1/3$, $p_2 = 0.6$, $w_3(x) = (5x + 7)/12$, $p_3 = 0.2$. A time series $\{x_i\}_{i=1}^{N_s}$, $N_s = 10^6$, associated with this process is generated by using the random iteration algorithm for IFSP (Barnsley, 1988),

$$x_{i+1} = w_h(x_i) \quad \text{Prob. } p_h. \quad (45)$$

Figure 6 shows the behavior of $\beta^{(\pm)}(x^*)$ vs. x^* for several randomly chosen values of x^* (the admissible values for the exponent β are given by $\beta_1 = 1.465$, $\beta_2 = 0.368$, $\beta_3 = 1.838$).

As expected, the values of $\beta^{(\pm)}(x^*)$ lie along three straight lines parallel to the x^* -axis.

It should be observed that, under the assumptions stated above (the support \mathcal{C} is an interval), the application of the Laplace transform does not enable us to obtain the values of the translation factors b_h . (The situation is slightly different when \mathcal{C} is a Cantor dust. In the latter case, information about b_h can be obtained from the Laplace transform method discussed earlier. For the sake of brevity, the study of this case is not reported here.) This is not a major problem, since in the understanding of the multiplicative structure, only the scaling factors a_h and the probability weights p_h control the statistics of physical observables.

In the case of nonlinear multiplicative processes, that is, in the presence of nonlinear transformations $w_h(x)$, the integral transform method can still be applied. The analysis of this case goes far beyond the aim of this article and will be developed elsewhere.

To sum up, the analysis developed in this subsection shows that integral transform theory can also be applied to address the identification problem of the multiplicative structure underlying AES distributions. This method applies both to initial (inlet) distributions (such as singular chromatograms) and to experimental (computer) data sets that are customarily studied in order to characterize the statistics of mixing processes (stretching exponents, curvatures, striation thicknesses).

Transport Schemes

From a physical standpoint, smooth distributions may be a rather oversimplified assumption, especially in connection with heterogeneous chemistry and transport processes involving solid adsorbents, catalysts, and porous structures. Heterogeneity occurs either in the structure of the complex diffusive paths experienced by diffusing species, or in the distribution of the catalytic activities and adsorption equilibrium constants (Sheintuch and Rebhun, 1988; Marczewski et al., 1990; Moon et al., 1991; Annesini et al., 1994).

This kind of problem has been considered by means of Monte Carlo simulations by Gutfraind et al. (1990, 1991) in connection with catalytic properties and scaling laws in the presence of a singular (multifractal) distribution of catalytic activities.

Continuous-mixture models of transport phenomena (chromatographic separations) have been studied by McCoy (1989), McCoy and Goto (1994), and Giona et al. (1994).

In order to highlight the application of AES distributions in transport phenomena, let us consider the case of a diffusional release of a continuous solute mixture, for example, from a swollen polymeric matrix, into an infinite reservoir in which solute concentration can be assumed to be practically vanishing. A similar model has been analyzed by Bailey (1975).

In the one-dimensional formulation, the transport scheme reads as

$$\frac{\partial c}{\partial t} = \mathcal{D}(x) \frac{\partial^2 c}{\partial z^2}$$

$$c|_{z=0} = 0, \quad \frac{\partial c}{\partial z} \Big|_{z=L} = 0, \quad c|_{t=0} = c_0(x) = c_0 \rho(x).$$
(46)

In this case, the modeling by means of a continuous parameter may have different physical interpretations:

- It can be related to the presence of a continuous mixture of solutes, each of which characterized by a different diffusivity $\mathcal{D}(x)$.

- It can be related to the release of a single solute from a highly heterogeneous matrix with a continuous distribution of diffusional paths, each of which is characterized by a different diffusivity (characteristic diffusional time).

In any case, regardless of the physical motivation underlying the continuous parametrization, it is convenient to take the continuous parameter x , proportional to the diffusivity, that is, $\mathcal{D}(x) = \mathcal{D}_{\max} x$.

By solving Eq. 46, the fractional solute release $\langle M_\theta \rangle / \langle M_\infty \rangle \langle \cdot \rangle$ indicates the average with respect to the initial distribution $\rho(x)$ up to the dimensionless time $\theta = \mathcal{D}_{\max} t / L^2$ can be expressed as

$$\frac{\langle M_\theta \rangle}{\langle M_\infty \rangle} = \frac{\int_{\mathcal{C}} dx \int_0^\theta x \frac{\partial c(z, \theta'; x)}{\partial z} \Big|_{z=0} d\theta'}{\int_{\mathcal{C}} dx \int_0^\infty x \frac{\partial c(z, \theta'; x)}{\partial z} \Big|_{z=0} d\theta'}$$

$$= \sum_{n=0}^{\infty} \frac{1}{\lambda_n^2} [1 - \mathcal{L}(\lambda_n^2 \theta)] \Big/ \sum_{n=0}^{\infty} \frac{1}{\lambda_n^2}, \quad (47)$$

where $\lambda_n = (n+1)\pi/2$, $n = 0, 1, \dots$, and $\mathcal{L}(\cdot)$ is the Laplace transform associated with the initial distribution $\rho(x)$.

Asymptotically, for large θ , the fundamental mode ($n=0$) controls the release, and therefore

$$1 - \frac{\langle M_\theta \rangle}{\langle M_\infty \rangle} \simeq \mathcal{L}(\lambda_0^2) \sim \theta^{-\beta}, \quad (48)$$

where the exponent β is related to the singularity structure of AES distributions through Eq. 18.

Let us investigate the intermediate scaling, that is, behavior of the uptake curve $\langle M_\theta \rangle / \langle M_\infty \rangle$ up a value of about 0.5–0.6. This is customarily the range investigated in controlled release experiments in connection with case II (also called anomalous) diffusion, for which a scaling exponent different from 1/2 can be observed experimentally in the scaling of the fractional uptake curve as a function of time (Crank, 1967).

Figure 7 shows the behavior of the normalized uptake curve associated with different AES (multifractal) initial distributions $\rho(x)$ (model I discussed, in the second section). As can be observed, regardless of the multifractal structure of the distribution, a regular behavior is observed in the uptake curve, that is, $\langle M_\theta \rangle / \langle M_\infty \rangle \sim \theta^{1/2}$.

This result should be compared with the recent analysis of Giona et al. (1996a,b,c) of uptake properties of fractal structures obtained by means of exact Green function renormalization, which shows that, on a fractal pore network, the uptake curve admits an anomalous behavior, $\langle M_\theta \rangle / \langle M_\infty \rangle \sim \theta^\omega$, where the exponent ω depends on the fractal dimension of the pore network, on the walk dimension of the structure, and also on the dimension of the exchange area with the external reservoir.

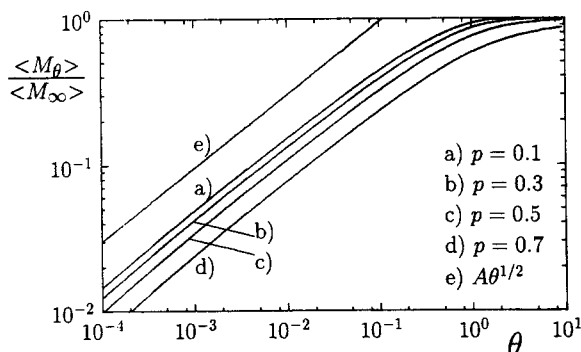


Figure 7. $\langle M_\theta \rangle / \langle M_\infty \rangle$ for the continuous release model, Eqs. 46–47 obtained for an initial binomial distribution (model I) of the diffusing species $c_o(x)$ for different values of p ; line (e) is the line $\langle M_\theta \rangle / \langle M_\infty \rangle = A\theta^{1/2}$, with $A = \text{constant}$.

This comparison clearly indicates that it is not possible to simulate anomalous diffusional transport by means of a superposition of parallel diffusional pathways, regardless of the singularity and heterogeneity of the diffusivities since the complex topology of the network plays a fundamental role. This is a further confirmation that the attempt to describe complex pore-network topology by means of parallel-bundle models, as so often applied in chemical engineering in the past, constitutes an intrinsically naive and nonrealistic approach.

Elliptic Equations with Singular Boundary Conditions

The theory of integral transforms can also be applied to solve basic equations of mathematical physics that are the fundamental background in the study of transport phenomena (Carslaw and Jaeger, 1959) in the presence of AES boundary conditions.

This section develops as a case study a simple but significant example, namely the solution of the Dirichlet problem for the Laplace equation on the circle. This is the simplest nontrivial problem for elliptic equations, which finds applications in the theory of steady-state transport phenomena, for example, heat-transfer (Carslaw and Jaeger, 1959).

Let us consider the Laplace equation,

$$\nabla^2 c = 0 \quad (49)$$

inside a circle of radius R , that is, for $r < R$, $\theta \in [0, 2\pi]$ equipped with the boundary conditions of Dirichlet type

$$c(R, \theta) = c_o(\theta). \quad (50)$$

The solution of this equation is referred to as the Poisson formula

$$c(r, \theta) = \frac{1}{2\pi} \int_0^{2\pi} K(r, \theta - \psi) c_o(\psi) d\psi, \quad (51)$$

where the Poisson kernel $K(r, \theta - \psi)$ is given by (Courant and Hilbert, 1962)

$$K(r, \theta - \psi) = \frac{1 - (r/R)^2}{1 - 2(r/R)\cos(\theta) + (r/R)^2} = 1 + 2 \sum_{n=1}^{\infty} \left(\frac{r}{R}\right)^n \cos[n(\theta - \psi)]. \quad (52)$$

By a change of variables, $\theta = 2\pi y$, $\psi = 2\pi \eta$ ($y, \eta \in [0, 1]$), $\xi = r/R$, $\tilde{c}_o(y) = c_o(2\pi y)$, the solution of the Dirichlet problem reads as

$$c(\xi, y) = \int_0^1 \tilde{c}_o(\eta) dy + 2 \sum_{n=1}^{\infty} \xi^n \int_0^1 \tilde{c}_o(\eta) \cos[2\pi(y - \eta)] d\eta. \quad (53)$$

Let us consider the case where $\tilde{c}_o(y)$ is proportional to an AES distribution μ on $[0, 1]$ $C_o d\mu(y) = \tilde{c}_o(y) dy$, where C_o is a positive constant. From Eq. 53 it follows that

$$c(\xi, y) = C_o \left[1 + 2 \sum_{n=1}^{\infty} \xi^n (\text{Re}[\Phi(2\pi n)] \cos(2\pi y) + \text{Im}[\Phi(2\pi n)] \sin(2\pi y)) \right], \quad (54)$$

where $\Phi(\omega) = \int \exp(I\omega y) d\mu(y)$ is the Fourier transform of μ , and can be expressed by Eqs. 13–15, with $s = -I\omega$.

Figure 8 shows the behavior of $c(\xi, y)$ vs. the angular coordinate y for different values of ξ , where μ is the invariant measure associated with a 3-map IFSP $w_i(x) = sx + b_i$ ($i = 1, 2, 3$), with $s = 1/3$, $b_1 = 0$, $b_2 = 1/3$, $b_3 = 2/3$ for $p_1 = 0.2$, $p_2 = 0.6$, $p_3 = 0.2$. As can be expected, the solution $c(\xi, y)$ becomes rougher as ξ increases up to the boundary. A measure of the roughening is given by the mean square deviation $\sigma^2(\xi) = \int_0^1 [c(\xi, y) - \langle c(\xi) \rangle]^2 dy$, with $\langle c(\xi) \rangle = \int_0^1 c(\xi, y) dy$. As can be expected from the Laplacian nature of the boundary-value problem, $\sigma^2(\xi) \sim \xi^2$, as confirmed by the analysis of the data (Figure 9).

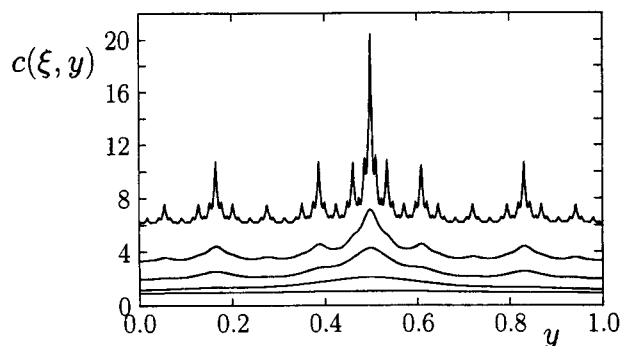


Figure 8. Behavior of $c(\xi, y)$ vs. y , Eq. 54 for different values of ξ (from bottom up, $\xi = 0.1, 0.5, 0.8, 0.9, 0.99$).

The $c(\xi, y)$ -profiles have been translated along the vertical axis by a constant factor (vertical scale is arbitrary) in order to achieve a better visual representation.

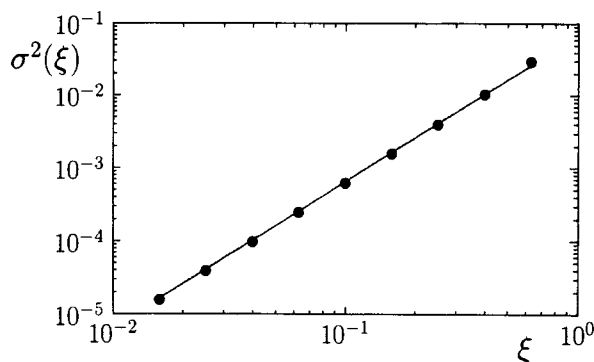


Figure 9. $\sigma^2(\xi)$ vs. ξ .

Dots are the data obtained from the solution of the Laplace equation, Eq. 54. The line is $\sigma^2(\xi) = A\xi^2$, with A constant.

To sum up, the simple case study developed in this section shows that the integral transform theory can be applied to solve partial differential equations in the presence of AES distributions. Other examples can be worked out within the theoretical framework of integral transform theory, since the solution of many other linear transport problems can be expressed in integral form through the introduction of the corresponding Green functions.

Concluding Remarks

In this article, which is mostly methodological, we have shown how it is possible to give a rigorous treatment of AES distributions in continuous kinetic modeling and in other chemical engineering applications.

In the case of AES distributions, the corresponding density $\rho(x)$ cannot be defined in a classic way. Nevertheless, the application of IFS theory makes it possible to obtain a rigorous definition of the average of any continuous functions, and especially of integral transforms such as the Laplace and Stieltjes transforms. In some respects, this is analogous to what happens for Dirac's delta distributions, which cannot be defined rigorously in terms of the standard calculus, but their integral properties are well posed within the theory of generalized functions.

The interest in AES distributions is fourfold:

- The analysis developed in this article shows that it is possible to develop a rigorous mathematical physics involving these distributions by taking advantage of their construction properties (IFS theory).
- AES distributions cover a gap between the limiting cases of atomic and smooth continuous distributions.
- The application of AES (multifractal) distributions is particularly interesting in heterogeneous catalysis as well as in many other industrial processes involving cascade and multiplicative processes, for example, in material manufacturing (particle breaking), turbulent eddy structures, mixing, and environmental issues (pollutant distributions).
- The theory of AES distributions may be a new and useful mathematical tool in order to develop a theory of mixing as discussed in the subsection titled "Reaction in Chaotic Mixing Systems." Indeed multifractal measures arise in connection with the distribution of stretching exponents in

chaotic mixing (Muzzio et al., 1992a,b). The analysis developed in this article for integral quantities can therefore be applied to new models of mixing with reaction for industrial and laboratory systems.

In particular, it has been observed by Gutfraind et al. (1991; see references therein) that experimental investigation of the equilibrium morphologies of metal crystallites influencing catalytic properties can be described in terms of fractal models leading to a multifractal distribution of catalytic activities.

In dealing with reaction/diffusion problems in disordered media, great care should be taken in developing models based on a continuous distribution of effective diffusion/reaction parameters, as this involves the assumption of the averaging and superposition of independent processes evolving in parallel. Network topology plays the leading role in all these cases and this assumption may therefore be intrinsically unacceptable.

A final remark concerns the problem of identifying AES distributions, which has already been approached in the literature in the case of unimodal IFS by means of the method of moments (Abenda and Turchetti, 1989; Bessis and Demko, 1991). The moment hierarchy $\{m_n\}$ associated with an AES distribution representing the invariant measure of a unimodal IFSP can be computed recursively by applying Eq. 7 to the function $f(x) = x^n$. By applying moment theory (Ahiezer and Krein, 1962), it is possible to approach the inverse identification problem, which consists of determining the parameters a_h , p_h , b_h , characterizing the distribution from the hierarchy of moments. For further details of the solution (and the limitations) of this inverse identification problem, see Abenda and Turchetti (1989) and Bessis and Demko (1991). The algorithmic approach to determine the scaling properties of AES distributions developed in the subsection on characterizing cascade processes seems to be a simpler and more powerful alternative to moment analysis.

Acknowledgments

The authors are deeply grateful to A. Adrover, M. Alvarez, S. Cerbelli, and F. J. Muzzio for useful discussions. One of the authors (M.G.) is grateful for the warm hospitality of the members of the Department of Chemical and Biochemical Engineering of the Rutgers University (NJ) and in particular of F. J. Muzzio.

Literature Cited

- Agenda, S., and G. Turchetti, "Inverse Problem for Fractal Sets on the Real Line via the Moment Method," *Il Nuovo Cimento*, **104 B**, 213 (1989).
- Annesini, M. C., M. Giona, and F. Gironi, "Continuous Model for Complex Mixture Adsorption," *Ind. Eng. Chem. Res.*, **33**, 2764 (1994).
- Ahiezer, N. I., and M. Krein, eds., *Some Questions in the Theory of Moments*, American Mathematical Society, Providence, RI (1962).
- Aris, R., "Reaction in Continuous Mixtures," *AIChE J.*, **35**, 539 (1989).
- Aris, R., "The Mathematics of Continuous Mixtures," *Kinetic and Thermodynamic Lumping of Multicomponent Mixtures*, G. Astarita and S. I. Sandler, eds., Elsevier, Amsterdam (1991).
- Aris, R., "Almost Discrete Γ -Distributed Chemical Species and Reactions," *Chem. Eng. Sci.*, **49**, 581 (1994).
- Aris, R., and G. R. Gavalas, "On the Theory of Reactions in Continuous Mixtures," *Philos. Trans. R. Soc. Lond.*, **A-260**, 351 (1966).
- Astarita, G., "Lumping Nonlinear Kinetics: Apparent Overall Order of Reaction," *AIChE J.*, **35**, 529 (1989).

- Astarita, G., and A. Nigam, "Lumping Nonlinear Kinetics in a CSTR," *AIChE J.*, **35**, 1927 (1989).
- Astarita, G., and R. Ocone, "Lumping Nonlinear Kinetics," *AIChE J.*, **34**, 1299 (1988).
- Astarita, G., and S. I. Sandler, eds., *Kinetic and Thermodynamic Lumping of Multicomponent Mixtures*, Elsevier, Amsterdam (1991).
- Bailey, J. E., "Diffusion and Grouped Multicomponent Mixtures in Uniform and Nonuniform Media," *AIChE J.*, **21**, 192 (1975).
- Barnsley, M., *Fractal Everywhere*, Academic Press, Boston (1988).
- Beigie, D., A. Leonard, and S. Wiggins, "Invariant Manifold Templates for Chaotic Advection," *Chaos Solitons Fractals*, **4**, 749 (1994).
- Bessis, D., and S. Demko, "Stable Recovery of Fractal Measures by Polynomial Sampling," *Physica D*, **47**, 427 (1991).
- Chou, M. Y., and T. C. Ho, "Continuum Theory for Lumping Nonlinear Reactions," *AIChE J.*, **34**, 1519 (1988).
- Chou, M. Y., and T. C. Ho, "Lumping Coupled Nonlinear Reactions in Continuous Mixtures," *AIChE J.*, **35**, 533 (1989).
- Carslaw, H. S., and J. C. Jaeger, *Conduction of Heat in Solids*, Clarendon Press, Oxford (1959).
- Courant, R., and D. Hilbert, *Methods of Mathematical Physics*, Vol. II, Wiley, New York (1962).
- Crank, J., *The Mathematics of Diffusion*, Clarendon Press, Oxford (1967).
- Falconer, K., *Fractal Geometry: Mathematical Foundations and Applications*, Wiley, New York (1990).
- Forte, B., and E. R. Vrsay, "Solving the Inverse Problem for Function/Image Approximation Using Iterated Function Systems: I. Theoretical Basis," *Fractals*, **2**, 325 (1994).
- Giona, M., "Integrals over Fractal Sets and Spatial Definition of Multifractality," *Chaos and Fractals in Chemical Engineering*, G. Biardi, A. R. Giona, and M. Giona, eds., World Scientific, Singapore, p. 293 (1995).
- Giona, M., M. Giustiniani, A. Adrover, and O. Patierno, "Nonlinear Reaction Diffusion Schemes in Continuous Kinetics," *Chem. Eng. Commun.*, **128**, 173 (1994).
- Giona, M., W. A. Schwalm, M. K. Schwalm, and A. Adrover, "Exact Solution of Linear Transport Equations in Fractal Media I—Renormalization Analysis and General Theory," *Chem. Eng. Sci.*, **51**, 4717 (1996a).
- Giona, M., W. A. Schwalm, M. K. Schwalm, and A. Adrover, "Exact Solution of Linear Transport Equations in Fractal Media II—Diffusion and Convection," *Chem. Eng. Sci.*, **51**, 4731 (1996b).
- Giona, M., A. Adrover, W. A. Schwalm, and M. K. Schwalm, "Exact Solution of Linear Transport Equations in Fractal Media III—Adsorption and Chemical Reaction," *Chem. Eng. Sci.*, **51**, 5065 (1996c).
- Grassberger, P., "Generalizations of the Hausdorff Dimension of Fractal Sets," *Phys. Lett.*, **107A**, 101 (1985).
- Gutfraind, R., M. Sheintuch, and D. Avnir, "Multifractal Scaling Analysis of Diffusion-limited Reactions with Devil's Staircase and Cantor Set Catalytic Structures," *Chem. Phys. Lett.*, **174**, 8 (1990).
- Gutfraind, R., M. Sheintuch, and D. Avnir, "Fractal and Multifractal Analysis of the Sensitivity of Catalytic Reactions to Catalyst Structure," *J. Chem. Phys.*, **95**, 6100 (1991).
- Halsey, T. C., M. H. Jensen, L. P. Kadanoff, I. Procaccia, and B. I. Shraiman, "Fractal Measures and Their Singularities: The Characterization of Strange Sets," *Phys. Rev. A*, **33**, 1141 (1986).
- Himmelblau, D. M., and K. B. Bishoff, *Process Analysis and Simulation*, Wiley, New York (1968).
- Ho, T. C., "Aggregate Behavior and Lumped Kinetics of Many Reactions in Backmixing and Plug-Flow Reactors," *AIChE J.*, **42**, 214 (1996).
- Ho, T. C., and R. Aris, "On Apparent Second-order Kinetics," *AIChE J.*, **33**, 1050 (1987).
- Levy-Vehel, J., "Fractal Approaches in Signal Processing," *Fractal Geometry and Analysis*, C. J. G. Evertsz, H.-O. Peitgen, and R. F. Voss, eds., World Scientific, Singapore (1996).
- Liu, M., and F. J. Muzzio, "The Curvature of Material Lines in Chaotic Cavity Flows," *Phys. Fluids*, **8**, 75 (1996).
- Liu, M., R. L. Peskin, F. J. Muzzio, and C. W. Leong, "Structure of the Stretching Field in Chaotic Cavity Flows," *AIChE J.*, **40**, 1273 (1994).
- Mandelbrot, B. B., "Intermittent Turbulence in Self-similar Cascade: Divergence of High Moments and Dimension of the Carrier," *J. Fluid Mech.*, **62**, 331 (1974).
- Mandelbrot, B. B., *The Fractal Geometry of Nature*, Freeman, San Francisco (1982).
- Mandelbrot, B. B., "An Introduction to Multifractal Distribution Functions," *Fluctuations and Pattern Formation*, H. E. Stanley and N. Ostrowsky, eds., Kluwer, The Netherlands (1988).
- Marczewski, A. W., A. Derylo-Marczewska, and M. Jaroniec, "A Simple Method for Describing Multi-Solute Adsorption Equilibria on Activated Carbons," *Chem. Eng. Sci.*, **45**, 143 (1990).
- McCoy, B. J., "Adsorption Chromatography of a Heterogeneous Mixture," *Chem. Eng. Sci.*, **44**, 993 (1989).
- McCoy, B. J., and M. Goto, "Continuous-Mixture Model of Chromatographic Separations," *Chem. Eng. Sci.*, **49**, 2351 (1994).
- Moon, H., H. C. Park, and C. Tien, "Adsorption of Unknown Substances from Aqueous Solutions," *Chem. Eng. Sci.*, **46**, 23 (1991).
- Moore, P. K., and R. G. Anthony, "The Continuous-lumping Method for Vapor-Liquid Equilibrium Calculations," *AIChE J.*, **35**, 1115 (1989).
- Muzzio, F. J., and J. M. Ottino, "Evolution of a Lamellar System with Diffusion and Reaction: A Scaling Approach," *Phys. Rev. Lett.*, **63**, 47 (1989a).
- Muzzio, F. J., and J. M. Ottino, "Dynamics of a Lamellar System with Diffusion and Reaction: Scaling Analysis and Global Kinetics," *Phys. Rev. A*, **40**, 7182 (1989b).
- Muzzio, F. J., C. Meneveau, P. D. Swanson, and J. M. Ottino, "Scaling and Multifractal Techniques for Analysis of Mixing in Chaotic Flows," *Phys. Fluids A*, **4**, 1439 (1992a).
- Muzzio, F. J., P. D. Swanson, and J. M. Ottino, "Mixing Distributions Produced by Multiplicative Stretching in Chaotic Flows," *Int. J. Bifurc. Chaos*, **2**, 37 (1992b).
- Ottino, J. M., *The Kinematics of Mixing: Stretching, Chaos and Transport*, Cambridge Univ. Press, Cambridge, England (1989).
- Pentek, A., T. Tel, and Z. Toroczka, "Fractal Tracer Patterns in Open Hydrodynamic Flows: The Case of Leapfrogging Vortex Pairs," *Fractals*, **3**, 33 (1995).
- Prigogine, I., and R. Herman, *Kinetic Theory of Vehicular Traffic*, (1971).
- Procaccia, I., "Fractal Structures in Turbulence," *J. Stat. Phys.*, **36**, 649 (1984).
- Sheintuch, M., and M. Rebhun, "Adsorption Isotherms for Multisolute Systems with Known and Unknown Composition," *Water Res.*, **22**, 421 (1988).
- Sreenivasan, K. R., and C. Meneveau, "The Fractal Facets of Turbulence," *J. Fluid Mech.*, **173**, 357 (1986).
- Vojak, R., "Analyse et Modélisation Multifractales de Signaux Complexes—Applications au trafic routier," PhD Thesis, Univ. de Paris IX Dauphine (1996).
- Vojak, R., and J. Levy-Vehel, "Predictability of Multiplicative Processes: A Preliminary Study," *Fractals*, **2**, 383 (1994).
- Vojak, R., J. Levy-Vehel, and M. Danech-Pajouh, "Multifractal Description of Road Traffic Structure," IFAC/IFORS Symp. on Transportation Systems: Theory and Applications of Advances Technology, Tianjin, China, p. 942 (1994).
- Wiggins, S., *Chaotic Transport in Dynamical Systems*, Springer-Verlag, Berlin (1992).
- Zou, H., G. Sheng, C. Sun, and O. Xu, "Distribution of Organic Contaminants in Lake Taihu," *Water Res.*, **30**, 2003 (1996).

Appendix 1

Let us consider a Borel measure μ on a compact support $\mathcal{C} \subset [0, 1]$, and a system $\{I_i(\epsilon)\}$ of intervals of diameter ϵ covering \mathcal{C} , their measure being $\mu(I_i(\epsilon))$.

The support \mathcal{C} can be subdivided into a union of subset \mathcal{C}_α such that

$$\mathcal{C}_\alpha = \left\{ x \in \mathcal{C} \mid \lim_{\epsilon \rightarrow 0} \frac{\log \mu(I(\epsilon))}{\log \epsilon} = \alpha \right\}, \quad (\text{A1})$$

where $I(\epsilon)$ is an interval belonging to $\{I_i(\epsilon)\}$ containing x , and α the Hölder exponent. Let $f(\alpha)$ be the fractal dimension of the set \mathcal{C}_α .

The graph $(\alpha, f(\alpha))$ is referred to as the *multifractal spectrum* of the measure.

In the case of invariant measures generated by means of unimodular IFSP, it can be proved (cf. Mandelbrot, 1988; Halsey et al., 1986) that the multifractal spectrum $f(\alpha)$ can be obtained from the auxiliary function $\tau(q)$, defined for $q \in (-\infty, \infty)$, as

$$\tau(q) = \frac{1}{\log a} \log \left(\sum_{h=1}^N p_h^q \right), \quad (\text{A2})$$

from the relations

$$\alpha(q) = \frac{\partial \tau(q)}{\partial q} \quad f[\alpha(q)] = q\alpha(q) - \tau(q). \quad (\text{A3})$$

The auxiliary function $\tau(q)$ is related to the spectrum of generalized dimension $D(q)$ (Grassberger, 1985) of μ through the relation

$$\tau(q) = (q-1)D(q). \quad (\text{A4})$$

In other words, in the scaling theory of multifractal measures, the support \mathcal{C} can be regarded as a union of subsets \mathcal{C}_α , $\mathcal{C} = \bigcup_\alpha \mathcal{C}_\alpha$, possessing fractal dimension $f(\alpha)$, each of which is characterized by a value α of the Hölder exponent.

Appendix 2

This Appendix develops the mathematical details related to the proof of the properties of integral transforms of AES distributions discussed throughout the article, and introduced in the third section.

Let us consider the Laplace transforms of invariant measures μ of affine IFSP. Without loss of generality we may assume that the transformations $w_h(x) = a_h x + b_h$ ($h = 1, \dots, N$) map $[0, 1]$ into itself and that $a_h > 0$. Moreover, let us order the map for increasing values of b_h , that is, $b_h < b_{h+1}$ and $b_1 = 0$.

The Laplace transform $\mathcal{L}(s)$ of μ satisfies the functional Eq. 11,

$$\mathcal{L}(s) = \sum_{h=1}^N p_h \exp(-sb_h) \mathcal{L}(a_h s) = \mathcal{K}[\mathcal{L}(s)], \quad (\text{A5})$$

with closure condition

$$\mathcal{L}(0) = 1. \quad (\text{A6})$$

The righthand side of Eq. A5 can be regarded as a functional operator $\mathcal{K}[\cdot]$ acting on $\mathcal{L}(s)$.

The Laplace transform $\mathcal{L}(s)$ is analytic (and bounded) in the half-plane of convergency $\text{Re}[s] > 0$.

Let us consider the functional $\mathcal{K}[\cdot]$ defined in the space of analytic functions $C_\infty(0)$ in the half-plane $\text{Re}[s] > 0$, equipped with the uniform metrics d_∞

$$d_\infty(f_2(s), f_1(s)) = \sup_s \|f_2(s) - f_1(s)\|$$

$$f_1, f_2 \in C_\infty(0), \quad (\text{A7})$$

where $\|\cdot\|$ is the modulus of a complex number and \sup_s indicates the supremum over s in the half-plane of convergency.

The functional $\mathcal{K}[\cdot]$ maps functions of $C_\infty(0)$ into functions of $C_\infty(0)$, that is, if $f_1(s) \in C_\infty(0)$, then $f_2(s) = \mathcal{K}[f_1(s)] \in C_\infty(0)$. For $f_1(s), f_2(s) \in C_\infty(0)$, the images $\mathcal{K}[f_1(s)], \mathcal{K}[f_2(s)]$ through the functional $\mathcal{K}[\cdot]$ satisfy the inequality

$$d_\infty(\mathcal{K}[f_2(s)], \mathcal{K}[f_1(s)])$$

$$= \sup_s \left\| \sum_{h=1}^N p_h \exp(-sb_h) [f_2(a_h s) - f_1(a_h s)] \right\| \leq d_\infty(f_2, f_1). \quad (\text{A8})$$

The functional $\mathcal{K}[\cdot]$ is not strictly a contraction, but due to its behavior is close to $s = 0$. Nevertheless, from Eq. (A8) it follows that the iteratives $f_{n+1}(s) = \mathcal{K}[f_n(s)]$ converge uniformly in $\text{Re}[s] > 0$.

In the particular case of unimodular IFSP (i.e., $a_h = a = \text{constant}$), let us consider the sequence of functions $\{L_n(s)\}$ defined by the relation

$$L_{n+1}(s) = \sum_{h=1}^N p_h \exp(-sb_h) L_n(as), \quad L_0(s) = 1. \quad (\text{A9})$$

The limit of this sequence exists, and is given by the converging infinite product $L_\infty(s)$

$$L_\infty(s) = \prod_{n=0}^{\infty} \left[\sum_{h=1}^N p_h \exp(-a^n b_h s) \right]. \quad (\text{A10})$$

It is a straightforward matter to show that the function $L_\infty(s)$ defined by Eq. A10 satisfies the functional Eq. A5, that is, $L_\infty(s) = \mathcal{K}[L_\infty(s)]$, and the closure condition Eq. A6, that is, $L_\infty(0) = 1$. This implies that $\mathcal{L}(s) = L_\infty(s)$. From Eq. A8 it follows that the sequence of iteratives $\{L_n(s)\}$ converges uniformly toward $L_\infty(s)$ in the half-plane $\text{Re}[s] > 0$. From Eq. A9 it follows that $L_n(s)$ can be expressed explicitly in the form of Eq. 14. By following the same approach, analogous properties of Fourier and Stieltjes transforms can be proved.

Let us now analyze the behavior of $\mathcal{L}(s)$ for large s (bearing in mind $b_1 = 0$ and $b_h < b_{h+1}$). The Laplace transform $\mathcal{L}(s)$ of invariant measures associated with affine IFSP shows for large $s \rightarrow \infty$ the behavior

$$\mathcal{L}(s) = As^{-\beta} + o(s^{-\beta}), \quad (\text{A11})$$

where A is a constant. In order to determine the exponent β , let us substitute Eq. A11 into Eq. A5,

$$As^{-\beta} = Ap_1 a_1^{-\beta} s^{-\beta} + o[s^{-\beta} \exp(-sb_2)]. \quad (\text{A12})$$

Therefore, for $s \rightarrow \infty$

$$1 = p_1 a_1^{-\beta}, \quad (\text{A13})$$

from which it follows that $\beta = \log p_1 / \log a_1$.

Manuscript received July 11, 1996, and revision received Dec. 31, 1996.